Developmental Biology 350 (2011) 548–558

Contents lists available at ScienceDirect

Developmental Biology

journal homepage: www.elsevier.com/developmentalbiology

Genomes & Developmental Control

TIF1β association with HP1 is essential for post-gastrulation development, but not for Sertoli cell functions during spermatogenesis

Marielle Herzog [a,b,c,d,e,1], Olivia Wendling [a,b,c,d,e], Florian Guillou [f], Pierre Chambon [a,b,c,d,e], Manuel Mark [a,b,c,d,e,g], Régine Losson [a,b,c,d,e,†], Florence Cammas [a,b,c,d,e,*]

[a] Institut de Génétique et de Biologie Moléculaire et Cellulaire (IGBMC), Illkirch-Cedex, France
[b] CNRS, Illkirch-Cedex, France
[c] INSERM, Illkirch-Cedex, France
[d] UdS, Illkirch-Cedex, France
[e] Collège de France, BP 10142, 67404 Illkirch-Cedex, France
[f] UMR 6175, Physiologie de la Reproduction, INRA/CNRS, Université de Tours, Haras Nationaux, F-37380 Nouzilly, France
[g] Hôpital Universitaire de Strasbourg 1, place de l'Hôpital, 67091 Strasbourg Cedex, France

ARTICLE INFO

Article history:
Received for publication 11 June 2010
Revised 17 November 2010
Accepted 6 December 2010
Available online 14 December 2010

Keywords:
HP1
TIF1β/KAP-1/TRIM28
Knock-in
Embryonic lethality
Nuclear organization
Chromatin
Mouse

ABSTRACT

TIF1β is an essential mammalian transcriptional corepressor. It interacts with the heterochromatin proteins HP1 through a highly conserved motif, the HP1box, and we have previously shown that this interaction is essential for the differentiation of F9 cells to occur. Here we address the *in vivo* functions of the TIF1β–HP1 interaction, by generating mice in which the TIF1β HP1box is mutated, leading to the loss of TIF1β interaction with HP1. The effects of the mutation were monitored in two instances, where TIF1β is known to play key roles: early embryonic development and spermatogenesis. We find that mutating the HP1box of TIF1β disrupts embryonic development soon after gastrulation. This effect is likely caused by the misexpression of TIF1β targets that regulate mitotic progression and pluripotency. In contrast, in Sertoli cells, we found that the absence of TIF1β but not its mutation in the HP1box leads to a clear defect of spermatogenesis characterized by a failure of spermatid release and a testicular degeneration. These data show that the interaction between TIF1β and HP1 is essential for some but not all TIF1β functions *in vivo*. Furthermore, we observed that TIF1β is dispersed through the nucleoplasm of E7.0 embryos, whereas it is mainly associated with pericentromeric heterochromatin of E8.5 embryos and of Sertoli cells, an association that is lost upon TIF1β HP1box mutation. Altogether, these data provide strong evidence that nuclear organization plays key roles during early embryonic development.

Introduction

The precise control of gene expression, cellular proliferation and differentiation are essential for organism to ensure their integrity and survival. During development, cell fate decisions are taken and tissue-specific gene expression patterns have to be established and maintained. The expression of pluripotency genes shuts down, the relevant tissue-specific genes become expressed, and the genes characteristic of other differentiation pathways become stably repressed (Mohn and Schübeler, 2009). There are increasing evidence that the structure of the chromatin and the organization of the nucleus play key roles in these events (for review Farnham, 2009; Takizawa et al., 2008). Of particular interest, heterochromatin, a sub-nuclear compartment long thought as an inert storage site for useless genetic information appears to be involved in several regulatory processes within the nucleus. However how these different levels of regulation are linked *in vivo* is still poorly understood.

One of the major components of heterochromatin is the heterochromatin protein 1 (HP1). HP1 proteins are highly conserved proteins found in organisms ranging from fission yeast to human; they play a crucial role in heterochromatin formation and contribute to the regulation of gene expression (Hiragami and Festenstein, 2005; Hediger and Gasser, 2006; Kwon and Workman, 2008). Mice and humans have three HP1 isotypes (α, -β, and -γ) which are not fully functionally redundant despite high structural and biochemical similarities (Aucott et al., 2008). All three proteins are comprised of an N-terminal chromodomain (CD) connected by a hinge region to a C-terminal chromoshadow domain (CSD). The CD specifically binds di- and trimethylated H3K9, the histone fold domain of H3, and methylated H1.4K26 (Bannister et al., 2001; Lachner et al., 2001; Nielsen et al., 2001; Daujat et al., 2005). The CSD is involved in self-association and also serves as a docking site for a variety of nuclear proteins implicated in transcriptional regulation, chromatin modification, replication, DNA

* Corresponding author. Institut de Génétique et de Biologie Moléculaire et Cellulaire (IGBMC), Illkirch-Cedex, France. Fax: +33 3 88 65 32 01.
E-mail address: Florence.cammas@igbmc.fr (F. Cammas).
[1] Present address: Laboratory of Cancer Epigenetics, Free University of Brussels, Faculty of Medecine, Route de Lennik, 808. B-1070 Brussels, Belgium.
† Deceased.

0012-1606/$ – see front matter © 2010 Elsevier Inc. All rights reserved.
doi:10.1016/j.ydbio.2010.12.014

repair, nuclear architecture and chromosomal maintenance (Brasher et al., 2000; Kwon and Workman, 2008; Dinant and Luijsterburg, 2009 and references therein). Thus, HP1 can be thought as bridging proteins, connecting histones through interactions with the CD, to diverse nuclear proteins, through interactions via their CSD. However, the mechanisms by which HP1 interactions regulate chromatin structure, gene expression, and ultimately cell fate are poorly understood.

Sequence comparison of a large number of HP1 partners identified the presence of a conserved PxVxL pentapeptide motif called HP1box, which is necessary and sufficient for their interaction with HP1 (Le Douarin et al., 1996; Murzina et al., 1999; Smothers and Henikoff, 2000). Specific amino acid changes within the HP1box have been identified that selectively disrupt interaction with HP1, thus providing tools to investigate the physiological relevance of this interaction (Thiru et al., 2004). For instance specific disruption of the PxVxL motif has revealed that the interaction between HP1 and the histone chaperone CAF1 is essential for the specific targeting of CAF1 to replication foci within heterochromatin, and for appropriate replication of this condensed chromatin structure (Quivy et al., 2008).

Among other well-established HP1-binding motif containing partners, the transcriptional intermediary factor 1 (TIF1) β (also named KAP-1 or TRIM28) exerts cellular functions essential for gastrulation and spermatogenesis in mice (Cammas et al., 2000; Weber et al., 2002). Initially identified through its ability to interact with the three mammalian HP1s (Le Douarin et al., 1996), TIF1β is also known as the essential corepressor for the large family of Krüppel-associated box (KRAB) zinc finger DNA binding proteins (Friedman et al., 1996; Abrink et al., 2001). Structurally, TIF1β consists of an N-terminal RING-B boxes-coiled coil (RBCC or tripartite) motif and a C-terminal PHD finger-bromodomain unit (see Fig. S1). Mechanistically, it displays characteristics of a molecular scaffold that coordinates the recruitment of histone modifying and remodeling activities required for the deposition of HP1, which in turn contributes to the stable formation of highly localized condensed chromatin structures that associate with pericentromeric heterochromatin to yield heritable gene silencing (Ayyanathan et al., 2003; Sripathy et al., 2006; Riclet et al., 2009). TIF1β has also recently been shown to be essential for silencing of retrotransposons through interaction with both KRAB-ZFPs and HP1 (Wolf and Goff, 2007, 2009; Wolf et al., 2008; Matsui et al., 2010; Rowe et al., 2010).

In mouse embryonic carcinoma F9 cells, the TIF1β HP1box is instrumental to the TIF1β euchromatin to heterochromatin relocation that accompanies primitive endodermal differentiation (Cammas et al., 2002) as well as to progression through terminal differentiation (Cammas et al., 2004). Although these data indicate that the heterochromatic and euchromatic compartments can communicate through HP1-directed nuclear compartmentalization of TIF1β, the actual role of TIF1β–HP1 interaction in TIF1β physiological and developmental functions still remains to be determined.

In the present study, we have assessed the functional relevance of the interaction between TIF1β and HP1 by genetically disrupting the TIF1β HP1box either in the whole mouse or specifically in Sertoli cells. We demonstrate that the integrity of the TIF1β HP1box is essential for early post-gastrulation development, whereas it is dispensable for TIF1β specific functions within Sertoli cells during spermatogenesis. Altogether our data suggest that the relocation of TIF1β from euchromatin to heterochromatin rather than its association *per se* to heterochromatin is important for TIF1β functions during differentiation.

Results

The TIF1β HP1box is essential for early post-gastrulation development

ES cells targeted by homologous recombination were used to generate mice carrying alleles of TIF1β mutated in the HP1box encoding sequence, designated hereafter, at the homozygous state, as *TIF1*β^{HP1box} mutants (Fig. S1; Cammas et al., 2004). *TIF1*$\beta^{HP1box/+}$ heterozygous mice, which were viable and fertile, were intercrossed. Mendelian ratios of wild-type (WT), *TIF1*$\beta^{HP1box/+}$ and *TIF1*β^{HP1box} embryos were observed up to embryonic day (E) 8.5 and 9.5 (Table 1). By E10.5, however, there were fewer *TIF1*β^{HP1box} homozygous mutants than predicted and all were dead (Table 1). At day E11.5, the homozygous mutant tissues that could be genotyped were necrotic. No *TIF1*β^{HP1box} mutant was ever recovered at, or after E12.5 (Table 1 and data not shown). Therefore, similar to the *TIF1*β null mutation (Cammas et al., 2000), the *TIF1*β^{HP1box} knock-in (KI) mutation causes recessive embryonic lethality.

Representative external and histological aspects of WT and *TIF1*β^{HP1box} mutants embryos collected at different times of gestation are displayed in Fig. 1A(a and b) and B(a–i). At the late gastrula stage (E7.0), *TIF1*β^{HP1box} mutants were indistinguishable from WT embryos, as they all exhibited three germ layers and normal extraembryonic structures (Fig. 1A(a–d)). Similar to WT embryos, *TIF1*β^{HP1box} mutants expressed the mesodermal marker *Brachyury* (compare Fig. 1A, e and f). At E8.5, however, *TIF1*β^{HP1box} mutants were markedly retarded (Fig. 1B, a and b), while at E9.5 their body size, number of somites (10–12), and organs (Fig. 1B, d and h) resembled those of E8.5 WT embryos (Fig. 1B, a and i). Moreover, E8.5 and E9.5 *TIF1*β^{HP1box} mutants constantly displayed abnormal cranial neural tube closure and embryonic turning (Fig. 1Bd). At E10.5, *TIF1*β^{HP1box} mutants were all dead, as assessed by the absence of heart beats (Fig. 1Bf and data not shown). Taken together, these results demonstrate that the HP1-binding domain of TIF1β is dispensable for mesoderm induction and gastrulation, but required shortly thereafter for early organogenesis.

The TIF1β HP1box is essential for cell cycle regulation during development

Growth retardation can result from altered cell death and/or cell proliferation. Apoptotic cell death, assessed by TUNEL assays, was not different between E7.5 WT and *TIF1*β^{HP1box} mutants (Fig. 2A) or between E8.5 WT and E9.5 *TIF1*β^{HP1box} mutants (data not shown). Cell proliferation was assessed at E7.5 by BrdU incorporation and detection of mitosis by immunostaining histological sections with an antibody to phosphorylated histone H3. A small, but significant, 1.3-fold decrease in the percentage of cells in S-phase was detected in *TIF1*β^{HP1box} mutants as compared to their WT littermates (Fig. 2B). In contrast, the number of cells in M-phase was significantly higher in *TIF1*β^{HP1box} mutants (Fig. 2C). In this respect, it is interesting to mention that we recently found that replacement of TIF1β by a TIF1β^{HP1box} mutant protein in F9 cells increases expression of the mitotic checkpoint *Pttg1* (*Pituitary Tumor-Transforming Gene 1*). *Pttg1* transcription was increased in both undifferentiated and in retinoic acid-treated *TIF1*$\beta^{HP1box/-}$ F9 cells, as compared to *TIF1*$\beta^{+/-}$ cells placed under identical culture conditions, and the amount of PTTG1,

Table 1
Genotype analysis of *TIF1*$^{HP1box/+}$ intercross progeny.

Stage	Genotype			Total
	+/+	HP1box/+	HP1box/HP1box	
Newborn	47	57	0	104
E 12.5	5	6	0	11
E 11.5	10	20	5** (14%)	35
E 10.5	11	17	7** (20%)	35
E 9.5	10	28	13* (25%)	51
E 8.5	24	60	27* (24%)	111

*Embryos are growth retarded.
**Embryos are dead and eventually partially resorbed.

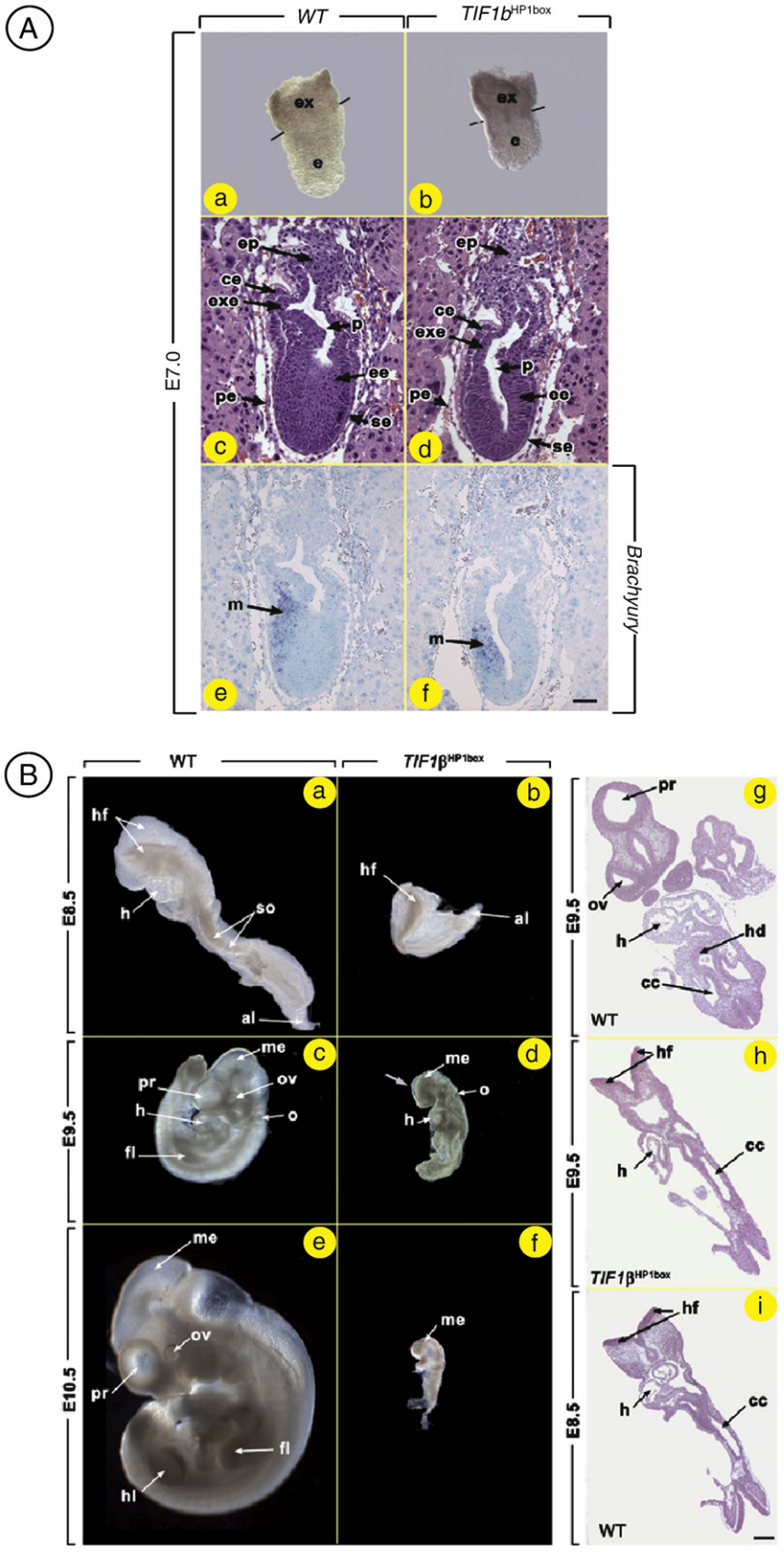
A
WT
Tlf1b HP1box
E7.0
ex
e
a
b
ep
ce
exe
p
ee
pe
se
c
d
m
e
f
Brachyury
B
WT
Tlf1β HP1box
E8.5
E9.5
E10.5
hf
h
so
al
me
pr
ov
o
fl
hl
cc
hd
g
h
i

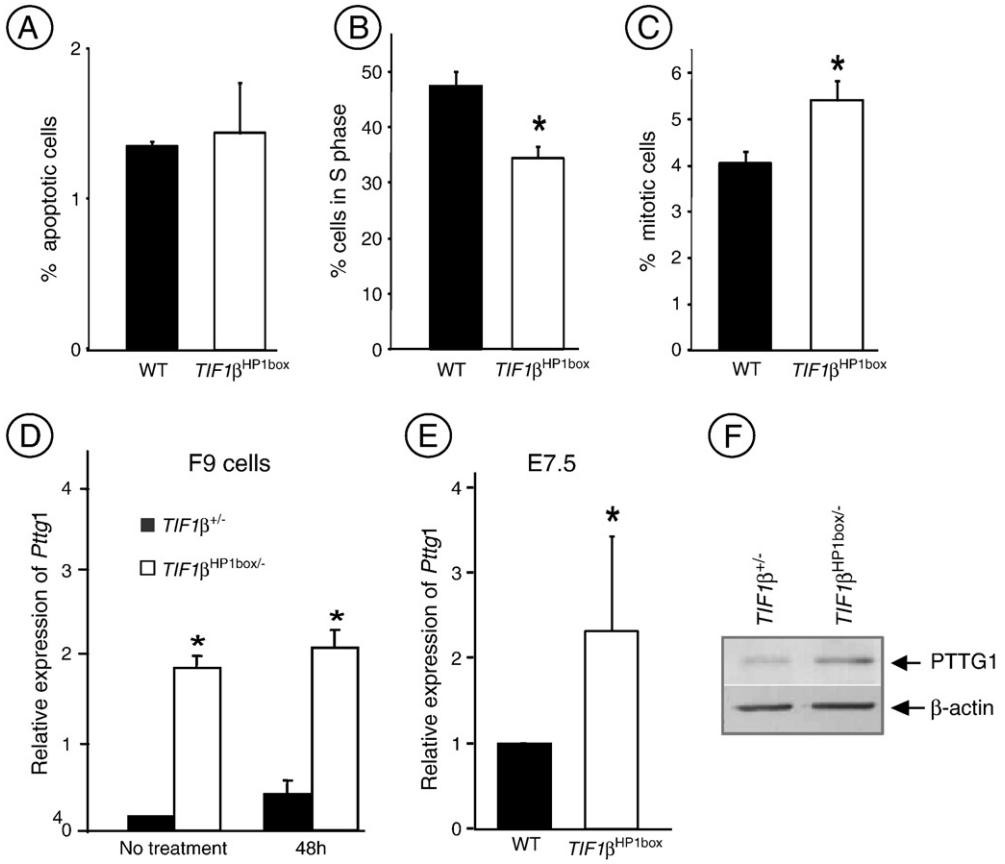

Fig. 2. Apoptosis and proliferation in *TIF1*β^{HP1box} mutants. (A) TUNEL-positive cells in WT (black bar) and *TIF1*β^{HP1box} mutant (white bar) embryos. (B) Quantification of proliferation after BrdU immunofluorescence analysis of E7.5 WT and *TIF1*β^{HP1box} mutant embryos. (C) Quantification of mitotic cells by immunostaining with anti-phosphorylated-histone H3 (PH3) antibody. The mean proportion (± SD) of positive cells was determined from sections of whole embryo and from three different embryos per genotype. Statistical significance was analyzed using Student's *t* tests (*, $P<0.05$; **, $P<0.01$). (D and E) RT-PCR analysis of *Pttg1* using RNA isolated from (D) *TIF1*β$^{+/-}$ and *TIF1*β$^{HP1box/-}$ F9 cells and (E) from E7.5 WT and *TIF1*β^{HP1box} littermates ($n=6$). Results are presented as expression relative to *Hprt*, with expression of *Pttg1* arbitrarily set equal to one for the WT samples. Each column represents the mean ± SD of at least three independent experiments (*, $P<0.05$; **, $P<0.005$). (F) Western blot analysis of PTTG1 expression in *TIF1*β$^{+/-}$ and *TIF1*β$^{HP1box/-}$ F9 cells synchronized in mitosis. Whole cell extracts (10 μg) from *TIF1*β$^{+/-}$ and *TIF1*β$^{HP1box/-}$ F9 cells treated with 0.12 μg/ml nocodazole for 24 h were resolved by SDS-PAGE and analyzed by immunoblotting with the monoclonal anti-TIF1β antibody 1 TB3 (Nielsen et al., 1999). β-Actin served as loading control.

measured by Western blotting, was increased in *TIF1*β$^{HP1box/-}$ cells synchronized in M-phase as compared to *TIF1*β$^{+/-}$ F9 cells (Fig. 2D and F and data not shown). These *in vitro* results encouraged us to investigate *Pttg*1 expression in E7.5 *TIF1*β^{HP1box} embryos. RT-PCR analysis showed a statistically significant 2.3-fold increase in the expression level of *Pttg1* in *TIF1*β^{HP1box} mutants as compared to their WT littermates (Fig. 2E). These data indicate that the TIF1β HP1box is essential for accurate control of *Pttg1* expression during embryonic development and suggest that *Pttg*1 over-expression could account for the abnormal cell cycle of *TIF1*β^{HP1box} mutants. Because the cell cycle regulator cyclin-dependent kinase inhibitor p21/CIP1/WAF1 (referred hereafter as p21) has already been proposed to be a TIF1β target gene and could have relevance in the proliferation defect observed in our mutant embryos, its expression was also verified at E7.5. Semi-quantitative RT-PCR analysis shows that, although p21 expression was quite variable between embryos, there was a 3.1-fold increased expression in mutant embryos as compared to their WT counterparts (Fig. S2). Taken together, the above results indicate that the integrity of the HP1box of TIF1β is required for proper cell cycle progression during embryonic development.

The TIF1β HP1box is essential for controlling Nanog and Oct4 expression

TIF1β was recently shown to play an important role in the pluripotency of ES cells (Hu et al., 2009). This led us to assess the expression of *Nanog* and *Oct4*, which are both required for the maintenance of stem cell pluripotency (reviewed by Chambers and Tomlinson, 2009). We analyzed *TIF1*β^{HP1box} mutant embryos at E6.5 which are morphologically normal and in which *Nanog* and *Oct4* expression levels are high and functionally relevant for the subsequent developmental steps (Chambers et al., 2003, 2007). Quantitative RT-PCR analysis revealed that expression of *Nanog* and *Oct4* was decreased by 2.7- and 3.8-fold respectively, in *TIF1*β^{HP1box} mutants as compared to WT embryos indicating that TIF1β interaction with HP1 is involved in the regulation of *Oct4* and *Nanog* expression (Fig. 3A and B).

Fig. 1. (A) *TIF1*β^{HP1box} mutants undergo gastrulation. (a,b) External aspect, (c,d) histological analysis and (e,f) *in situ* hybridization analysis of *Brachyury* expression of E7.0 wild-type (WT) and *TIF1*β^{HP1box} mutant littermates. Abbreviations: ce, cuboidal visceral endoderm; e and ex, embryonic and extraembryonic portions of the conceptus (separated by black lines); ee, embryonic ectoderm; ep, ectoplacental cone; exe, extraembryonic ectoderm; m, mesoderm; p, proamniotic cavity; pe, parietal endoderm; se, squamous visceral endoderm. Bar (in F): 560 μm (a, b), 50 μm (c–f). See also Fig. S1. (B) *TIF1*β^{HP1box} mutation delays embryonic development by E8.5. (a,b), (c,d) and (e,f) External aspect of WT and *TIF1*β^{HP1box} mutant littermates at E8.5, E9.5 and E10.5, respectively. (g and h) Representative histological sections of E9.5 WT and *TIF1*β^{HP1box} mutant embryos. (i) Histological sections of WT embryos at E8.5 are comparable to sections of mutant embryos at E9.5. Abbreviations: al, allantois; cc, coelomic cavity; fl, forelimb bud; h, heart; hd, hepatic diverticulum; hf, head fold; hl, hindlimb bud; me, mesencephalon; o, otocyst; ov, optic vesicle; pr, prosencephalon; so, somites; the arrow points to the failure of neural tube closure (d). Bar (in I): 200 μm (a–bb), 900 μm (c–f), 110 μm (g–i).

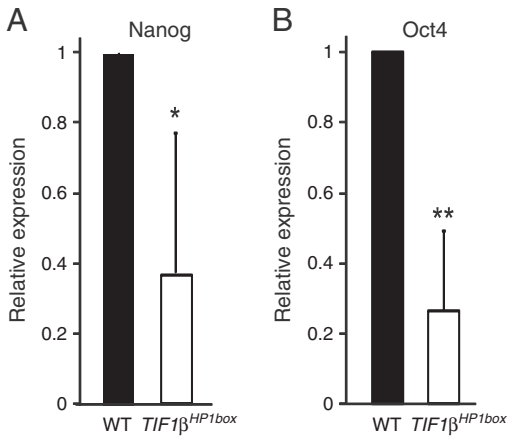

Fig. 3. Integrity of the TIF1β HP1box is required for appropriate embryonic expression of *Nanog* and *Oct4*. RT-PCR analysis of (A) *Nanog* and (B) *Oct4* expression using RNA isolated from WT and *TIF1*β^{HP1box} littermates ($n=6$) at E6.5 Results are presented as expression relative to *Hprt*, with expression of *Nanog* and *Oct4* arbitrarily set equal to one for the WT samples. (*, $P<0.05$; **, $P<0.005$).

TIF1β relocates from eu- to heterochromatin during early embryonic development

As the early embryonic lethality of *TIF1*β^{HP1box} mutants indicated an indispensable function for the HP1-binding activity of TIF1β, we analyzed the sub-nuclear localization of TIF1β by immunohistochemistry on sections of E7.0 and E8.5 embryos and used a DAPI counterstain as a marker of pericentromeric heterochromatin. TIF1β was expressed throughout the embryonic tissues (Fig. 4A–D). Confocal microscopy analysis of WT embryos at E7.0 showed that TIF1β was diffusely distributed within the nucleoplasm in a majority of nuclei (Fig. 4B, arrowhead), whereas at E8.5 it displayed a pericentromeric localization in virtually all cells (Fig. 4D). Importantly, the association of TIF1β with heterochromatin was not observed in E8.5 *TIF1*β^{HP1box} mutants (compare Fig. 4E and F with Fig. 4G and H). These results demonstrate that TIF1β relocates from euchromatin to heterochromatin shortly after gastrulation in an HP1box-dependent manner.

To determine whether the disruption of the interaction between TIF1β and HP1 had consequences on HP1 localization and on heterochromatin organization on its whole, we analyzed HP1α localization in WT and *TIF1*β^{HP1box} embryos. As shown on Fig. 5, HP1α was expressed at equivalent levels and displays the same sub-nuclear localization in both WT and *TIF1*β^{HP1box} embryos. Altogether these results demonstrate that the disruption of the interaction between TIF1β and HP1 specifically leads to the exclusion of TIF1β from heterochromatin without any detectable consequences on HP1 and heterochromatin organization.

Specific TIF1β gene targeting in Sertoli cells

Next, we investigated the role of TIF1β and its interaction with HP1 in cells that were already committed to specific lineages. We decided (i) to ablate *TIF1*β or (ii) to mutate the TIF1β HP1box in the testicular Sertoli cells (SC) which act as supporting cells for the male germ cell lineage.

To this end we made use of the *Amh-Cre* transgenic mouse line in which the Cre recombinase expression is regulated by the anti-Müllerian hormone promoter which is active only in SC (*Amh-Cre*$^{tg/0}$ line; Lécureuil et al., 2002). We produced mice having TIF1β inactivated specifically in SC (thereafter called *TIF1*β$^{Sc-/-}$) and mice with TIF1β HP1box mutated specifically in SC (thereafter called *TIF1*β$^{ScHP1box/-}$; see Materials and methods). The presence and the sub-nuclear distribution of TIF1β in SC were analyzed in each aforementioned mouse line by confocal immunofluorescence microscopy. In 7-week-old males, SC are terminally differentiated with respect to cell polarity, G0 arrest and ability to support the differentiation of functional spermatozoa. In testes of WT mice and *TIF1*β$^{Sc+/-}$ mutants, TIF1β was unevenly distributed with an intense pericentromeric heterochromatin staining and a weak, diffuse, nucleoplasmic staining in all SC (Fig. 6A–C and G–I and Weber et al., 2002). As expected TIF1β staining was absent specifically within Sertoli cells of *TIF1*β$^{Sc-/-}$ animals demonstrating the complete Sertoli cell-specific inactivation of TIF1β (Fig. 6D–F and data not shown). In contrast, in SC of *TIF1*β$^{ScHP1box/-}$ testes, the TIF1β^{HP1box} protein was distributed throughout the nucleoplasm with the exclusion of the pericentromeric heterochromatin (Fig. 6J–L). We also assessed the localization of HP α, β and γ in the different genetic backgrounds. As in embryos, the levels of expression and the sub-nuclear localization of the different HP1 isoforms were very similar in *TIF1*β$^{ScL2/L2}$, *TIF1*β$^{Sc-/-}$ and *TIF1*β$^{ScHP1box/-}$ Sertoli cells (Figs. S3–S5). These results indicate that the HP1-binding motif of TIF1β is essential for its pericentromeric heterochromatin association in SC, whereas it does not influence HP1 localization.

TIF1β but not its HP1box is essential for Sertoli cell functions

Mutant and control mice were analyzed for testis weight and testis to body weight ratios at different ages after puberty [i.e. at 7 weeks (W7) and 12 months (M12) of age]. Body weights were similar in WT, *TIF1*β$^{Sc-/-}$, *TIF1*β$^{Sc+/-}$ and *TIF1*β$^{ScHP1box/-}$ mice at all ages (data not shown). However, testis weights were reduced by 51% ($P<0.004$) and 70% ($P < 0.004$), respectively, in *TIF1*β$^{Sc-/-}$ mutants at W7 and M12 as compared to their WT littermates (Fig. S6; $n=4$ in each age group of WT or *TIF1*β$^{Sc-/-}$ mice). In marked contrast, there was no significant difference in testis weights between *TIF1*β$^{ScHP1box/-}$ mutants and *TIF1*β$^{Sc+/-}$ control mice (Fig. S6; $n=4$ in each group). To investigate fertility, *TIF1*β$^{Sc-/-}$ and WT males were mated with WT C57/Bl6 females for 5 months. *TIF1*β$^{Sc-/-}$ males produced significantly less litter per cage [3 ± 2.18 (mean ± SD, $n=9$)], than WT males [7.75 ± 1.71 ($n=4$; $p<0{,}001$)]. Moreover, the mean number of newborns per litter was significantly reduced in matings involving *TIF1*β$^{Sc-/-}$ males (3.3 ± 2.6) as compared to those involving WT males (7.6 ± 0.9; $p<0.001$). These results indicate that the *TIF1*β$^{Ser-/-}$ males are hypofertile.

Histological analysis of testes and epididymides was performed in young (W7, $n=10$) as well as aged (M12, $n=4$) mice. All *TIF1*β$^{Sc-/-}$ mutants had normal SC as assessed by hematoxylin and eosin and DAPI staining (Figs. 6 and 7 and data not shown) indicating that TIF1β is not involved in the maintenance of the Sertoli cell morphology. Nine out of the 10 *TIF1*β$^{Ser-/-}$ mutants at W7 displayed an abnormal testicular histology characterized by a decreased number of mature spermatids (S16, compare Fig. 7A and D), that failed to become aligned at the luminal side of the seminiferous tubules at stage VII of the epithelial cycle (see Russell et al., 1990 for a description of the epithelial stages). Moreover, mature spermatids were retained within the seminiferous epithelium and therefore were still present at epithelial stages IX and X, instead of being normally released at stages VII to VIII indicative of a spermiation defect (S16r; Fig. 7E). In agreement with these observations, the caudal epididymides of *TIF1*β$^{Sc-/-}$ mutants contained only few spermatozoa (Z, compare Fig. 7C and F). Old *TIF1*β$^{Sc-/-}$ mutants displayed, in addition to a failure of spermatid release, a testicular degeneration manifested by (i) a marked reduction in the diameters of the seminiferous tubules (T, compare Fig. 7G and J), (ii) frequent desquamation of immature germ cells (i.e., round spermatids; not shown), (ii) the presence of vacuoles in the seminiferous epithelium (arrowhead in Fig. 7K), and (iii) the existence of seminiferous tubules markedly depleted in germ cells or lined only by SC (Fig. 7K and data not shown). In contrast to *TIF1*β$^{Sc-/-}$ mutants, the testes from *TIF1*β$^{ScHP1box/-}$ mutants analyzed by histology at W7 ($n=4$) and M12 ($n=4$) were indistinguishable from those of age-matched *TIF1*β$^{Sc+/-}$ control mice (Fig. 7M and N), and accordingly their caudal epididymides contained abundant spermatozoa stores (Fig. 7O).

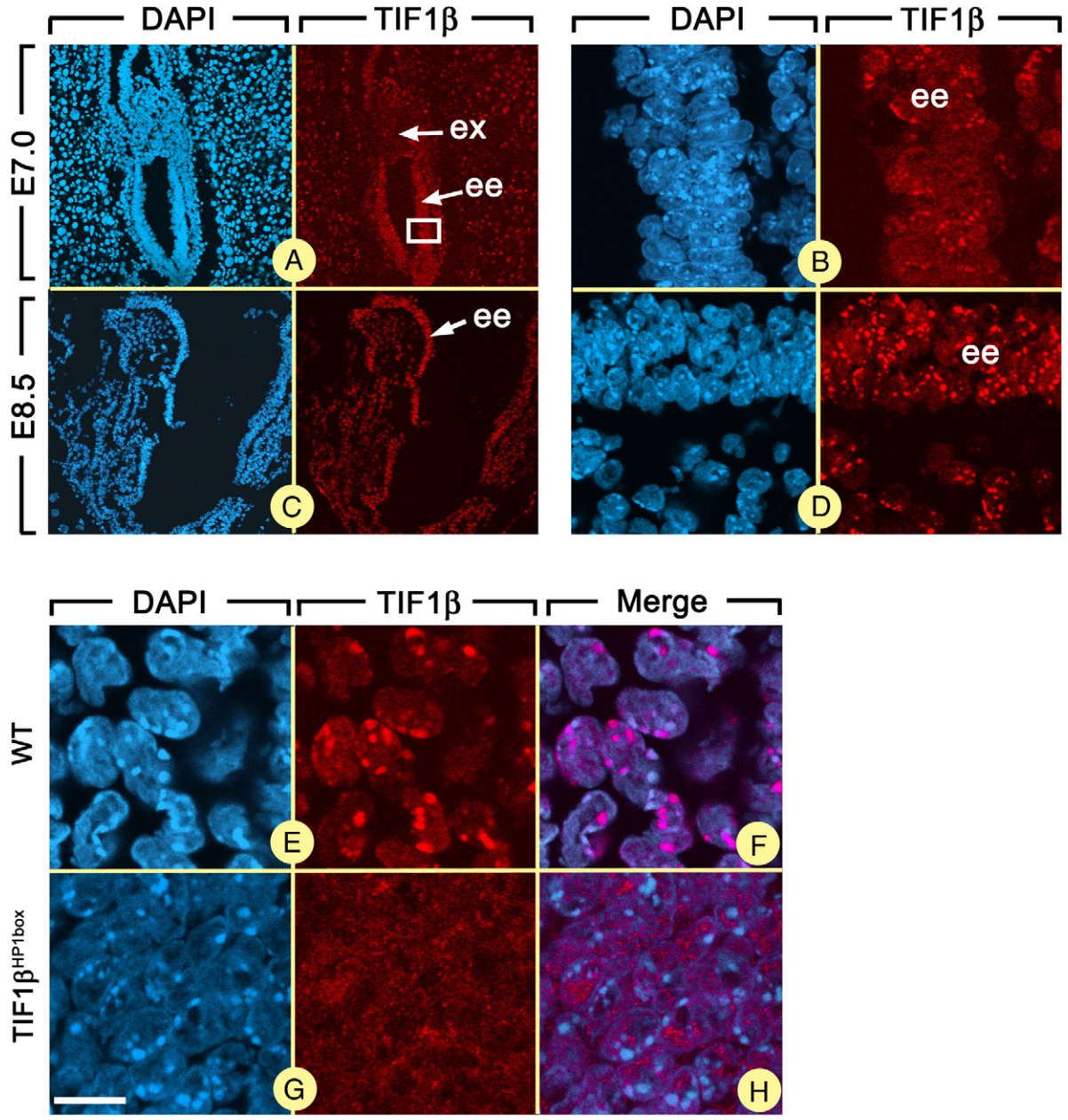

Fig. 4. TIF1β undergoes sub-nuclear redistribution during early post-gastrulation development in a HP1-binding domain-dependent manner. (A–D) Confocal microscopic analysis of TIF1β expression (red signals) in WT embryos at E7.0 (A and B) and E8.5 (C and D). Note that (B) and (D) represent high magnifications of the boxes in (A) and (C) respectively and that the DAPI counterstaining (blue signal) of the immunostained sections, highlights A/T-rich repeat sequences present in the centromeric heterochromatin (bright blue patches). (E–H) Comparative confocal microscopic analysis of the sub-nuclear localization of TIF1β in the ectoderm of E8.5 WT (E and F) and *TIF1β*^{HP1box} mutant (G and H) littermates. Abbreviations: ex, extraembryonic tissue; ee, embryonic ectoderm. Scale bar: 200 μm (A–C), 30 μm (B–D), 15 μm (E–H).

The number of SC in adult testis determines its size, as each SC has the capacity to support survival and differentiation of only a limited number of germ cells (Sharpe et al., 2003). Therefore, both the reduction in testis size and the germ cell depletion observed in *TIF1β*$^{Sc-/-}$ mutant mice could be accounted for by a reduced number of SC. As only immature SC proliferate, the total number of SC populating the adult testis is established before sexual maturity, around 3 weeks after birth (Vergouwen et al., 1993). Using 5-bromodeoxyuridine (BrdU) incorporation, we determined the rate of SC proliferation in testes at 5 day postpartum (P5), a stage when SC divide very actively. No significant differences in the percentage of BrdU-positive SC were observed between WT (24.5 ± 2.3%; $n = 4$) and *TIF1β*$^{Sc-/-}$ testes (28.9 ± 2.4%; $n = 4$). Furthermore, the ratio of Sertoli cells to spermatogonia in *TIF1β*$^{Sc-/-}$ mutants and WT testes, 4.7 ± 0.7 and 6 ± 1.2, respectively, was not statistically different (Fig. S7B). These results indicate that the absence of TIF1β in SC does neither alter SC nor spermatogonia proliferation (Fig. S7).

Altogether these results indicate that TIF1β is not required for SC morphological differentiation but plays an essential role in their spermatogenetic functions. Indeed TIF1b is determinant within SC for spermiation and for the maintenance of the seminiferous epithelium. We further demonstrate that the integrity of the HP1box or TIF1β association to heterochromatin is required for TIF1β SC-specific functions.

Discussion

In this study we demonstrate unambiguously that *in vivo* TIF1β acts through different mechanisms: one that is critically dependent upon its interaction with HP1 while others are not.

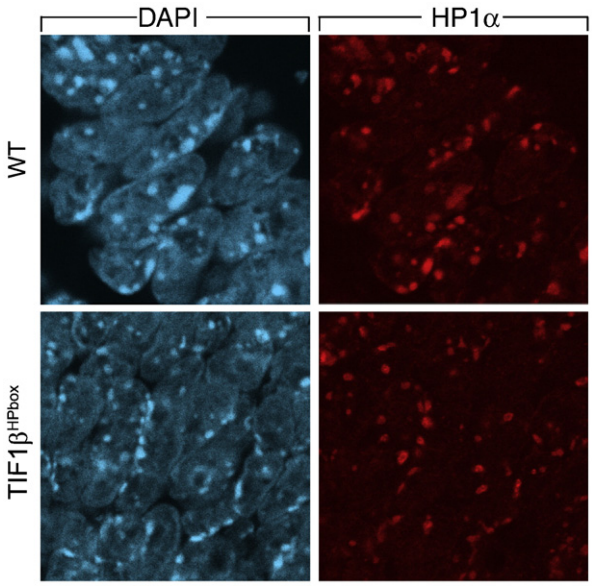

Fig. 5. The expression and localization of HP1α is not affected by TIF1β HP1box mutation. Confocal microscopic analysis of HP1α (red signals) and of DAPI counter-staining (blue signal) in E8.5 WT and *TIF1β*^{HP1box} embryos. Scale bar: 15 μm.

Requirement of the TIF1β HP1box during early embryonic development

We show that TIF1β HP1box mutation in mice leads to early developmental arrest shortly after gastrulation. Considering the recent literature and our own unpublished data, TIF1β binds to more than 3000 sites within mouse chromatin (O'Geen et al., 2007; Hu et al., 2009 and data not shown). Thus, it is likely that the inability of *TIF1β*^{HP1box} embryos to develop beyond E8.5 results from multifactorial effects. We have nevertheless identified molecular and cellular defects that may, in part, explain this lethality. Firstly, we found that *Nanog* and *Oct4* expression is decreased in E6.5 *TIF1β*^{HP1box} embryos, as compared to their WT littermates. Both genes have been shown to play crucial roles in the maintenance of the pluripotent status of ES cells (reviewed by Chambers and Tomlinson, 2009). Furthermore, *Nanog* inactivation in the mouse leads to a developmental arrest prior to gastrulation, suggesting that its decreased expression in *TIF1β*^{HP1box} mutant embryos could be responsible for their developmental arrest (Mitsui et al., 2003). Intriguingly, TIF1β has been reported to directly bind to both NANOG itself and to the regulatory sequence within the *Nanog* gene (Wang et al., 2006; Loh et al., 2007; Hu et al., 2009). Our finding that the disruption the TIF1β HP1box results in decreased *Nanog* expression suggests that the TIF1β/HP1 complex could positively regulate *Nanog* expression. The possibility that of a molecular complex with known functions in transcriptional repression could also be involved in transcriptional activation is not unprecedented, as the Sin3A/HDAC corepressor complex also plays a direct positive role in the regulation of *Nanog* expression through interaction with the transcription factor Sox2 (Baltus et al., 2009). Secondly, we find that the number of mitotic cells is significantly increased in the mutant embryos as compared to WT, suggesting a defect in chromosome segregation. Interestingly, we found that the mitotic checkpoint PTTG1 is more abundant in E7.5 *TIF1β*^{HP1box} embryos than in WT littermates. PTTG1 is involved in the regulation of sister chromatid separation during the mitotic phase of the cell cycle (reviewed by Cohen-Fix, 2001) and accumulation of PTTG1 protein has been shown to disrupt mitotic progression and to inhibit growth in cultured cells (Ying et al., 2006; Mu et al., 2003). It is therefore possible that the altered progression of *TIF1β*^{HP1box} mutant cells through mitosis is a direct consequence of increased expression of PTTG1 and could be involved in *TIF1β*^{HP1box} mutant embryos developmental arrest. Furthermore, Swi6 the yeast ortholog of HP1 itself is known to be involved in chromosome segregation in yeast by being involved in sister chromatid cohesion (Ekwall et al., 1995; Bernard et al., 2001). Finally, we found that the p21 is up-regulated in *TIF1β*^{HP1box} as compared to WT embryos. This result is consistent with the report that p21 is a direct target of TIF1β through binding of the KRAB-ZFP protein ZBRK1 within the p21 promoter region (Lee et al., 2007). P21 is well known to be involved in the regulation of cell cycle progression and in differentiation, suggesting that its increased expression could participate to *TIF1β*^{HP1box} embryos phenotype.

Some TIF1β functions are independent of its interaction with HP1

Up to now, all TIF1β functions as transcriptional corepressor were shown to require interaction between TIF1β and HP1, but whether the disruption of this interaction leads to complete or strong but partial loss of TIF1β repression activity, is a matter of debate (Ayyanathan et al., 2003; Wolf et al., 2008; Riclet et al., 2009). In the case of a partial loss, TIF1β target genes would still be repressed by a mutated TIF1β lacking the HP1box, albeit less efficiently than by TIF1β, resulting in milder phenotype than those observed upon complete inactivation of TIF1β. Another, non-mutually exclusive possibility would be that some of TIF1β functions could be completely independent of its interaction with HP1. Several studies support this latter possibility. For instance, TIF1β was reported to function as coactivator of several proteins including the transcription factors C/EBPβ (Chang et al., 1998) and NGFI-B/Nur77 (Rambaud et al., 2009), the coactivators TRIP-Br1 (Hsu et al., 2001), STAT3 (Tsuruma et al., 2008) and Oct4 (Seki et al., 2010). TIF1β was also shown to modulate the activity of p53 and E2F1 through involvement in their post-translational modifications (Wang et al., 2005, 2007; Tian et al., 2009). These functions are unlikely to require the interaction between TIF1β and HP1 and could account for the phenotypic differences resulting from TIF1β inactivation and TIF1β HP1box mutation. Furthermore, a detailed genome-wide approach comparing TIF1β binding sites to sites enriched in the H3K9 tri-methylated mark well known to be recognized by HP1 showed only 25% overlap, strongly suggesting that HP1 is not present on the remaining 75% TIF1β binding sites, and therefore that TIF1β-mediated regulation of many genes could be independent of its interaction with HP1 (O'Geen et al., 2007).

TIF1β targeting to, but not maintenance within heterochromatin is essential for TIF1β functions

We show here that TIF1β associates with heterochromatin of E8.5 embryonic cells as well as with that of SC, and that this association requires the TIF1β HP1box. As this relocation occurs at a developmental stage when *TIF1β*^{HP1box} embryos start to be growth-retarded it is very likely to be physiologically relevant. Interestingly, in these two *in vivo* models, disruption of the interaction between TIF1β and HP1 occurs at different steps with respect to TIF1β association with heterochromatin. In the case of the TIF1β HP1box germ-line mutation, the interaction between TIF1β and HP1 is already impaired prior to the time when TIF1β becomes normally associated with heterochromatin. In contrast, in the case of the SC-specific TIF1β HP1box mutation, interaction between TIF1β and HP1 is only impaired at a time when TIF1β is already associated with heterochromatin (data not shown). Thus, the effect of the TIF1β HP1box mutation is detrimental to TIF1β functions when the interaction between TIF1β and HP1 is disrupted prior to normal targeting of TIF1β to heterochromatin, as here during embryonic development and as previously reported for early differentiating F9 cells (Cammas et al., 2004). On the other hand, when the TIF1β HP1box mutation is induced after the normal time of TIF1β association with heterochromatin, as here in SC and as previously shown for retinoic acid-induced primitive endodermal cells (Cammas et al., 2004), the mutation leads to TIF1β dissociation from heterochromatin but has no effect on TIF1β functions. It

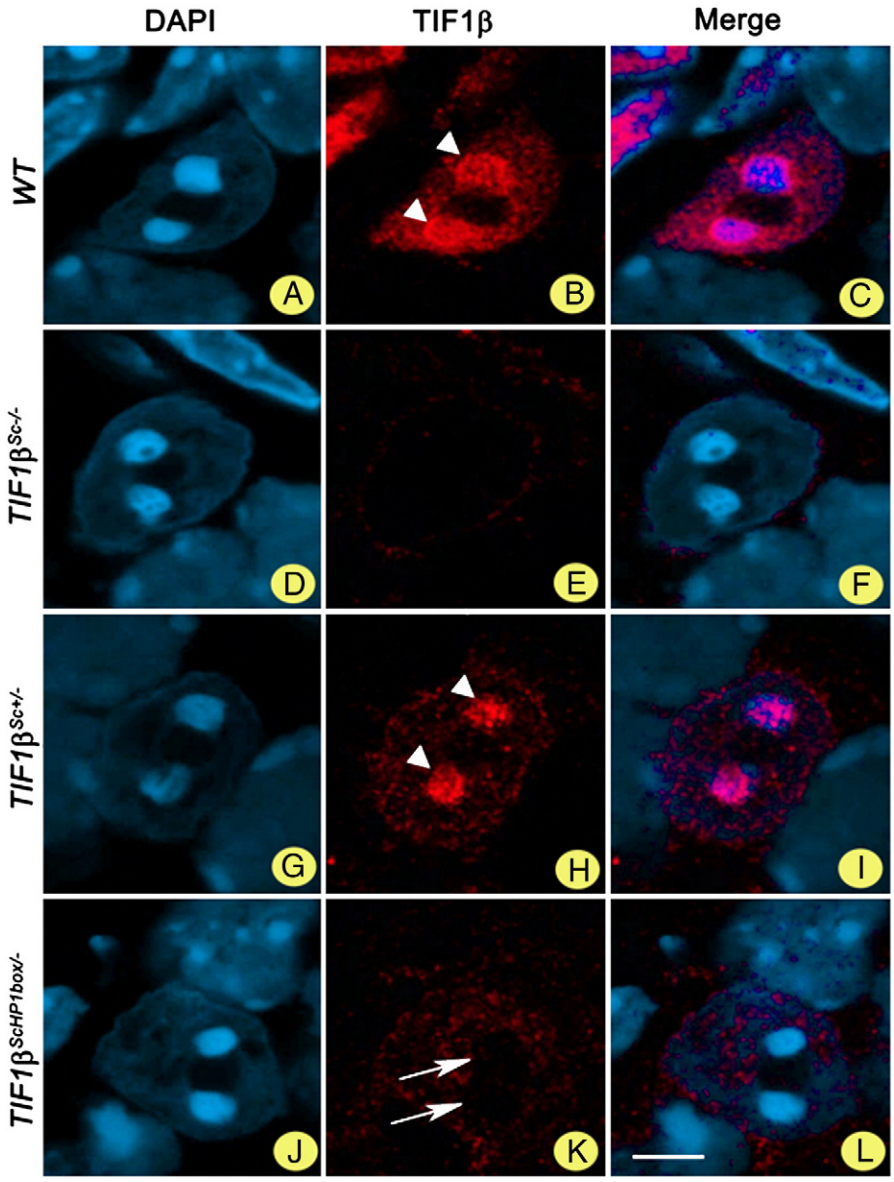

Fig. 6. Mutation of TIF1β HP1box prevents its association with pericentromeric heterochromatin in SC of post-pubertal testes. Frozen histological sections were incubated with the anti-TIF1β antibody and revealed with a Cy3-conjugated secondary antibody (red signal) and nuclei were counterstained with DAPI (blue signal). (B, E, H, and K) Cy3 and (A, D, G, and J) DAPI labeling. (C, F, I, and L) Superimposition of the two fluorochromes. (A–L) Confocal images of single optical sections through the SC nucleus of wild-type (A–C), *TIF1*$\beta^{Sc-/-}$ (D–F), *TIF1*$\beta^{Sc+/-}$ (G–I), and *TIF1*$\beta^{ScHP1box/-}$ (J–L) testes. In WT and *TIF1*$\beta^{Sc+/-}$ SC, TIF1β is preferentially associated with the pericentromeric heterochromatin organized in chromocenters (arrowheads). No immunostaining for TIF1β is detected in *TIF1*$\beta^{Sc-/-}$ mutant SC. In *TIF1*$\beta^{ScHP1box/-}$ mutant SC, TIF1β is diffusely distributed throughout the nucleoplasm, but excluded from the pericentromeric heterochromatin (arrows). Scale bar, 2 μm.

is therefore likely that the heterochromatic relocation of TIF1β in differentiating cells is instrumental to TIF1β functions, whereas the maintenance of this heterochromatic localization is dispensable. The function of the association of TIF1β to heterochromatin remains to be elucidated. However one can postulate that it could be important for tethering of TIF1β target genes to heterochromatin for stable silencing. This possibility is supported by our previous observation that in F9 cells, the association between TIF1β and HP1 facilitates the recruitment of the TIF1β target gene *MEST* to pericentromeric heterochromatin (Riclet et al., 2009). It is also possible that the TIF1β–HP1 complex participates to the formation of a chromatin structure only required at a specific stage of the differentiation process. Other examples of such differentiation stage specific regulation have been shown. Indeed, DNA methylation of specific genes, such as pluripotency and germ-line specific genes, occurs mainly during loss of pluripotency that accompanies the change from ES cells to progenitor cells. In contrast, there is almost no difference of DNA methylation between progenitor cells and terminally differentiated cells (Mohn et al., 2008). We have previously shown that TIF1β–HP1 association is involved in DNA methylation of MEST, a TIF1β target gene (Riclet et al., 2009). It is therefore conceivable that TIF1β–HP1 is specifically involved in TIF1β target genes regulated by DNA methylation *in vivo* and that this function is only required for a limited window of time during cell differentiation.

Materials and methods

ES cell selection

ES cells were electroporated with pTIF1β$^{LHL:HP1box}$ containing the PxAxA mutation in the HP1box domain of TIF1β (Cammas et al., 2004). Hygromycin resistant clones with homologous recombination of a single copy of the targeting vector as assessed by Southern blot with two

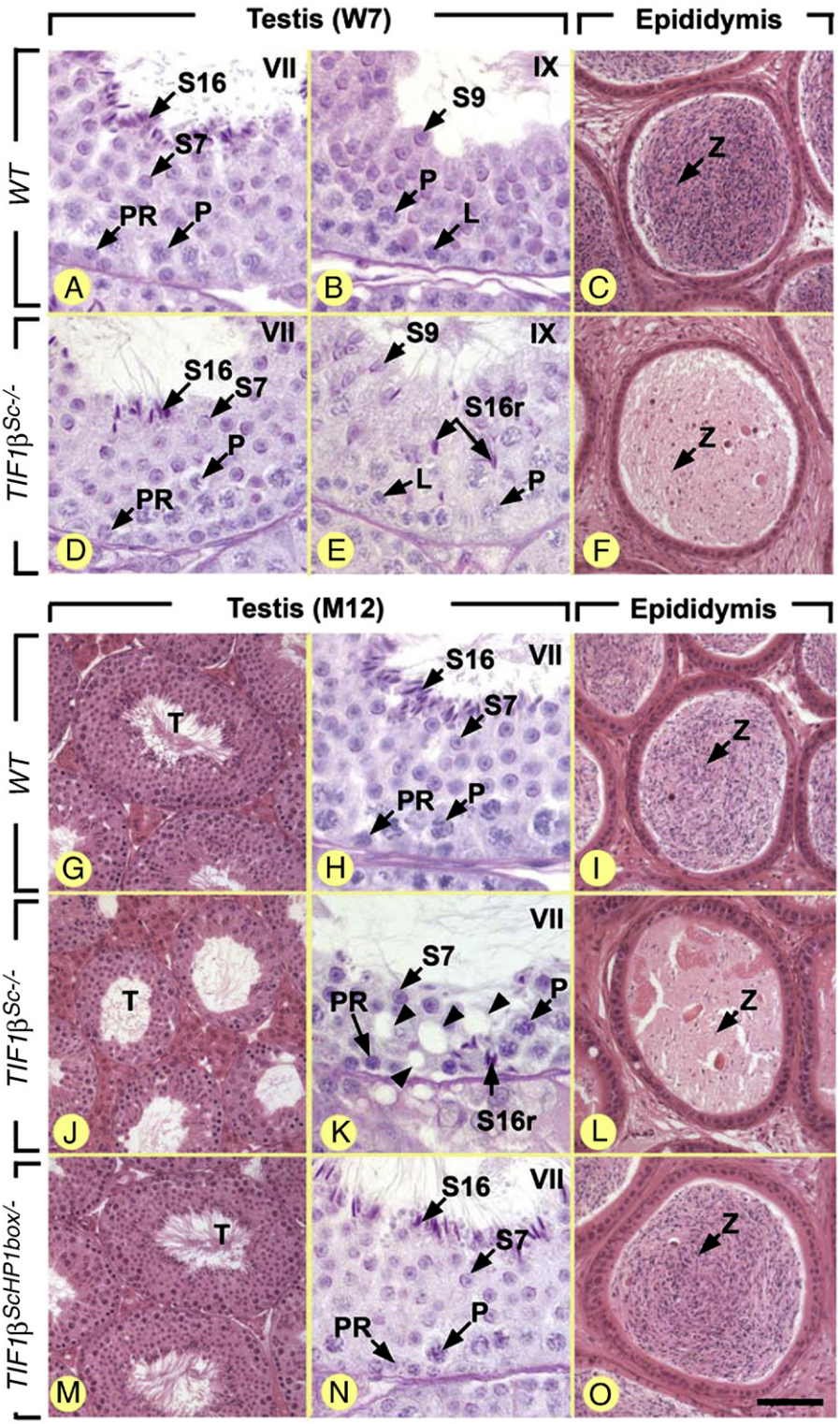

Fig. 7. Spermatogenesis and spermiation are impaired in *TIF1*$\beta^{Sc-/-}$, but not in *TIF1*$\beta^{ScHP1box/-}$ mutant mice. (A–O) Representative histological sections of testes (A, B, D, E, G, H, J, K, M, and N) and epididymides (C, F, I, L, and O) at W7 and M12 stained with hematoxylin and eosin (C, F, G, I, J, L, M, and O) or with periodic acid-Schiff (A, B, D, E, H, K, and N). Genotypes as indicated. Note that the sections displayed on a given line were obtained from the same mouse. L, leptotene spermatocytes; P and PR, pachytene and preleptotene spermatocytes, respectively; S7, S9, and S16, spermatids at steps 7, 9, and 16 of their maturation, respectively; S16r, retained step 16 spermatids; T, seminiferous tubule lumens; Z, spermatozoa. Arrowheads point to vacuoles in the seminiferous epithelium. Roman numerals designate stages of the seminiferous epithelium cycle. Scale bar (in O): 20 μm (A, B, D, E, H, K, and N) and 50 μm (C, F, G, I, J, L, M, and O). See also Figs. S2 and S3.

different probes (5' and hygro probes, Cammas et al., 2004) were selected. These clones were further analyzed for the incorporation of the HP1box mutation by PCR with primers flanking the HP1box motif: VR216 and TV211, followed by digestion with *Eco47*III, (Cammas et al., 2004) and called *TIF1*$\beta^{L2HP1box/+}$. The karyotype of these ES cells was verified by metaphase spreading.

Generation of mutant mice

*TIF1*β$^{L2HP1box/+}$ ES cells were used to derive *TIF1*β$^{HP1box/+}$ mice that were then intercrossed. Genotypes of the offspring were determined by PCR on genomic DNA extracted from tails (newborn, adult mice), from yolk sac (E8.5 to E12.5) or from paraffin-embedded sections with primers surrounding the site of insertion of the *LoxP* site (YD208, VR211; Cammas et al., 2000, 2004) or by PCR on cDNA detecting the HP1box mutation as described above. To generate SC-specific *TIF1*β knock-out mice, mice carrying *loxP*-flanked (floxed) alleles of *TIF1*β (*TIF1*β$^{L2/L2}$; Cammas et al., 2000) were crossed with mice bearing the *Amh-cre* transgene (Lécureuil et al., 2002) to generate *TIF1*β$^{L2/+}$:*Amh-Cre*$^{tg/0}$ mice. These mice were then crossed with *TIF1*β$^{L2/L2}$ mice to generate *TIF1*β$^{L2/L2}$:*Amh-Cre*$^{tg/0}$ males; these mice were referred to as *TIF1*β$^{Sc-/-}$ null mutants. These crosses also generated *TIF1*β$^{L2/L2}$:*Amh-Cre*$^{0/0}$ control males, which did not display histological defects and were thus referred to as wild-type (WT) mice. To generate SC-specific knock-in mice expressing only the mutant TIF1β^{HP1box} protein, *TIF1*β$^{HP1box/+}$ and *Amh-Cre*$^{tg/0}$ were first intercrossed to produce *TIF1*β$^{HP1box/+}$:*Amh-Cre*$^{tg/0}$ males. These mice were then crossed with *TIF1*β$^{L2/L2}$ mice to generate *TIF1*β$^{HP1box/L2}$:*Amh-Cre*$^{tg/0}$ males; these mice were referred to as *TIF1*β$^{ScHP1box/-}$ knock-in mutants. These crosses also generated *TIF1*β$^{HP1box/L2}$:*Amh-Cre*$^{0/0}$ and *TIF1*β$^{L2/+}$:*Amh-Cre*$^{tg/0}$ control males, which did not display histological defects. Genotypes were determined by genomic PCR on DNA extracted from tails using a mixture of three primers TV210, VR211 and YD208 for the wild-type, deleted, floxed and knock-in *TIF1*β alleles as previously described (Cammas et al., 2000, 2004) and a mixture of two primers TK139 (5′-ATTGCCTGCATTACCGGTC-3′) and TK141 (5′-ATCAACGTTTTGTTTTCGGA-3′) for the *Amh-Cre* transgene. All animal procedures were approved by the French Ministry of Agriculture (agreement B67-218-5) according to guidelines that are in compliance with the European legislation on care and use of laboratory animal.

Immunofluorescence and confocal microscopy analyses

Immunohistochemical detection of TIF1β was performed on 8 μm thick cryosections hydrated in phosphate-buffered saline (PBS), and then post-fixed in 4% paraformaldehyde (PFA) in PBS for 10 min at 4 °C. Sections were rinsed in PBS containing 0.1% Triton X-100 (PBST; 3×5 min at room temperature), saturated with 5% normal horse serum in PBST for 30 min at room temperature, and incubated with the anti-TIF1β polyclonal antibody (PF64; 4 μg/ml, Cammas et al., 2002) overnight at 4 °C. Sections were washed in PBST (3×5 min), incubated for 1 h at room temperature with the secondary antibody (Cy3-conjugated anti-rabbit IgG; diluted 1:400 in PBS, Jackson Laboratories), washed in PBST (3×5 min) and mounted in Vectashield® (Vector) containing DAPI at 10 μg/ml. Image acquisition was performed using a Leica TCS-4D confocal scanning microscope (Leica Microsystems, Heidelberg, Germany).

Histological analysis and detection of apoptotic cells

For histological analysis, embryos or testes were fixed in Bouin's fluid for 48 h, embedded in paraffin, sectioned at a thickness of 5 μm, and stained with either hematoxylin and eosin or periodic acid-Schiff. For detection of apoptotic cells, testes were perfusion-fixed with 4% PFA in PBS, whereas embryos were fixed within their decidua Testes and decidua were then maintained in this fixative for 16 h at 4 °C, and embedded in paraffin. TUNEL assay was performed on histological sections of three mutant and WT littermates using the ApopTag® Fluorescein Direct *In Situ* Apoptosis Detection kit according to the manufacturer's instructions (MP Biomedicals). Total cell numbers were determined by DAPI staining. The mean proportion (± SD) of TUNEL-positive cells was determined from 8 to 13 sections per embryo representing the whole embryo. Statistical analysis was carried out using Student's *t* tests.

BrdU incorporation and immunodetection of phosphorylated histone H3

To detect cells in S-phase, 5-bromo-2′-deoxyuridine (BrdU; Sigma) (100 mg/kg of body weight) was injected i.p. in pregnant *TIF1*β$^{HP1box/+}$ females or in males. Mice were sacrificed 2 h later; embryos or testis were collected and fixed in 4% paraformaldehyde (PFA) at 4 °C for 12 h, embedded in paraffin and processed for immunohistochemistry. The sections were incubated with an anti-BrdU antibody [Sigma; diluted 1:500 in PBS containing 0.05% Tween (PBST)] for 16 h at 4 °C, revealed with Cy3-conjugated goat anti-mouse IgG diluted 1:400 in PBST for 1 h at room temperature, and mounted in Vectashield® containing DAPI. Detection of mitotic cells was carried out using an anti-phosphorylated histone H3 (Ser10) antibody (Chemicon) diluted 1:1000 in PBST for 16 h at 4 °C. Statistical analysis was carried out using Student's *t* tests.

RT-PCR analysis

RNA extraction on single embryo was performed with a Trizol® (Invitrogen) solution according to the manufacturer's protocol. RNA was redissolved in 12 μl RNAse-free water. Reverse transcription (RT) was performed according to the manufacturer's specification (Superscript II RT; Invitrogen) adapted to minute amounts using an oligo(dT)$_{15}$ and a mixture of two enzymes: Superscript II (Invitrogen) and AMV-RT (Roche) (1:1). PCR were performed in a LightCyclerTM (Roche). The PCR primers used for amplification are available upon request. All quantifications were normalized to endogenous control HPRT.

Fertility assays

Seven-week-old *TIF1*β$^{Ser-/-}$ and control males were bred with fertile WT C57BL/6 females for up to 5 months. The number of litters produced and pups per litter were counted for each female.

Supplementary materials related to this article can be found online at doi:10.1016/j.ydbio.2010.12.014.

Acknowledgments

We thank M. Cervino for technical assistance as well as the staff of ES cell culture, the ICS and IGBMC animal facilities, the histopathology and embryology service and the Imaging Centre Technology platform. This work was supported by funds from the CNRS, the INSERM, the Association pour la Recherche sur le Cancer (ARC), and the Agence Nationale de la Recherche (ANR06-BLAN-0377). M.H. was supported by the Ministère de la Recherche et du Travail and ARC fellowships.

References

Abrink, M., Ortiz, J.A., Mark, M., Sanchez, C., Looman, C., Hellman, L., Chambon, P., Losson, R., 2001. Conserved interaction between distinct Kruppel-associated box domains and the transcriptional intermediary factor 1 β. Proc. Natl Acad. Sci. 98, 1422–1426.

Aucott, R., Bullwinkel, J., Yu, Y., Shi, W., Billur, M., Brown, J.P., Menzel, U., Kioussis, D., Wang, G., Reisert, I., Weimer, J., Pandita, R.K., Sharma, G.G., Pandita, T.K., Fundele, R., Singh, P.B., 2008. HP1-beta is required for development of the cerebral neocortex and neuromuscular junctions. J. Cell Biol. 183, 597–606.

Ayyanathan, K., Lechner, M.S., Bell, P., Maul, G.G., Schultz, D.C., Yamada, Y., Tanaka, K., Torigoe, K., Rauscher III, F.J., 2003. Regulated recruitment of HP1 to a euchromatic gene induces mitotically heritable, epigenetic gene silencing: a mammalian cell culture model of gene variegation. Genes Dev. 17, 1855–1869.

Baltus, G.A., Kowalski, M.P., Tutter, A.V., Kadam, S., 2009. A positive regulatory role for the mSin3A-HDAC complex in pluripotency through Nanog and Sox2. J. Biol. Chem. 284, 6998–7006.

Bannister, A.J., Zegerman, P., Partridge, J.F., Miska, E.A., Thomas, J.O., Allshire, R.C., Kouzarides, T., 2001. Selective recognition of methylated lysine 9 on histone H3 by the HP1 chromo domain. Nature 410, 120–124.

Bernard, P., Maure, J.F., Partridge, J.F., Genier, S., Javerzat, J.P., Allshire, R.C., 2001. Requirement of heterochromatin for cohesion at centromeres. Science 294, 2539–2542.

Brasher, S.V., Smith, B.O., Fogh, R.H., Nietlispach, D., Thiru, A., Nielsen, P.R., Broadhurst, R.W., Ball, L.J., Murzina, N.V., Laue, E.D., 2000. The structure of mouse HP1 suggests a unique mode of single peptide recognition by the shadow chromo domain dimer. EMBO J. 19, 1587–1597.

Cammas, F., Mark, M., Dollé, P., Dierich, A., Chambon, P., Losson, R., 2000. Mice lacking the transcriptional corepressor TIF1β are defective in early postimplantation development. Development 127, 2955–2963.
Cammas, F., Oulad-Abdelghani, M., Vonesch, J.L., Chambon, P., Losson, R., 2002. Cell differentiation induces TIF1β association with centromeric heterochromatin through HP1 interaction. J. Cell Sci. 115, 3439–3448.
Cammas, F., Herzog, M., Lerouge, T., Chambon, P., Losson, R., 2004. Association of the transcriptional corepressor TIF1β with Heterochromatin Protein 1 (HP1): an essential role for progression through differentiation. Genes Dev. 18, 2147–2160.
Chambers, I., Tomlinson, S.R., 2009. The transcriptional foundation of pluripotency. Development 136, 2311–2322.
Chambers, I., Colby, D., Robertson, M., Nichols, J., Lee, S., Tweedie, S., Smith, A., 2003. Functional expression cloning of Nanog, a pluripotency sustaining factor in embryonic stem cells. Cell 133, 643–655.
Chambers, I., Silva, J., Colby, D., Nichols, J., Nijmeijer, B., Robertson, M., Vrana, J., Jones, K., Grotewold, L., Smith, A., 2007. Nanog safeguards pluripotency and mediates germline development. Nature 450, 1230–1234.
Chang, C.J., Chen, Y.L., Lee, S.C., 1998. Coactivator TIF1beta interacts with transcription factor C/EBPbeta and glucocorticoid receptor to induce alpha1-acid glycoprotein gene expression. Mol. Cell. Biol. 18, 5880–5887.
Cohen-Fix, O., 2001. The making and breaking of sister chromatid cohesion. Cell 106, 137–140.
Daujat, S., Zeissler, U., Waldmann, T., Happel, N., Schneider, R., 2005. HP1 binds specifically to Lys26-methylated histone H1.4, whereas simultaneous Ser27 phosphorylation blocks HP1 binding. J. Biol. Chem. 280, 38090–38095.
Dinant, C., Luijsterburg, M.S., 2009. The emerging role of HP1 in the DNA damage response. Mol. Cell. Biol. 29, 6335–6340.
Ekwall, K., Javerzat, J.P., Lorentz, A., Schmidt, H., Cranston, G., Allshire, R., 1995. The chromodomain protein Swi6: a key component at fission yeast centromeres. Science 269, 1429–1431.
Farnham, P.J., 2009. Insights from genomic profiling of transcription factors. Nat. Rev. Genet. 10, 605–616.
Friedman, J.R., Fredericks, W.J., Jensen, D.E., Speicher, D.W., Huang, X.P., Neilson, E.G., Rauscher III, F.J., 1996. KAP-1, a novel corepressor for the highly conserved KRAB repression domain. Genes Dev. 10, 2067–2078.
Hediger, F., Gasser, S.M., 2006. Heterochromatin protein 1: don't judge the book by its cover! Curr. Opin. Genet. Dev. 16, 143–150.
Hiragami, K., Festenstein, R., 2005. Heterochromatin protein 1: a pervasive controlling influence. Cell. Mol. Life Sci. 62, 2711–2726.
Hsu, S.I., Yang, C.M., Sim, K.G., Hentschel, D.M., O'Leary, E., Bonventre, J.V., 2001. TRIP-Br: a novel family of PHD zinc finger- and bromodomain-interacting proteins that regulate the transcriptional activity of E2F-1/DP-1. EMBO J. 20, 2273–2285.
Hu, G., Kim, J., Xu, Q., Leng, Y., Orkin, S.H., Elledge, S.J., 2009. A genome-wide RNAi screen identifies a new transcriptional module required for self-renewal. Genes Dev. 23, 837–848.
Kwon, S.H., Workman, J.L., 2008. The heterochromatin protein 1 (HP1) family: put away a bias toward HP1. Mol. Cells 26, 217–227.
Lachner, M., O'Carroll, D., Rea, S., Mechtler, K., Jenuwein, T., 2001. Methylation of histone H3 lysine 9 creates a binding site for HP1 proteins. Nature 410, 116–120.
Le Douarin, B., Nielsen, A.L., Garnier, J.M., Ichinose, H., Jeanmougin, F., Losson, R., Chambon, P., 1996. A possible involvement of TIF1α and TIF1β in the epigenetic control of transcription by nuclear receptors. EMBO J. 15, 6701–6715.
Lécureuil, C., Fontaine, I., Crepieux, P., Guillou, F., 2002. Sertoli and granulosa cell-specific Cre recombinase activity in transgenic mice. Genesis 33, 114–118.
Lee, Y.K., Thomas, S.N., Yang, A.J., Ann, D.K., 2007. Doxorubicin down-regulates Kruppel-associated box domain-associated protein 1 sumoylation that relieves its transcription repression on p21WAF1/CIP1 in breast cancer MCF-7 cells. J. Biol. Chem. 282, 1595–1606.
Loh, Y.H., Zhang, W., Chen, X., George, J., Ng, H.H., 2007. Jmjd1a and Jmjd2c histone H3 Lys 9 demethylases regulate self-renewal in embryonic stem cells. Genes Dev. 21, 2545–2557.
Matsui, T., Leung, D., Miyashita, H., Maksakova, I.A., Miyachi, H., Kimura, H., Tachibana, M., Lorincz, M.C., Shinkai, Y., 2010. Proviral silencing in embryonic stem cells requires the histone methyltransferase ESET. Nature 464, 927–931.
Mitsui, K., Tokuzawa, Y., Itoh, H., Segawa, K., Murakami, M., Takahashi, K., Maruyama, M., Maeda, M., Yamanaka, S., 2003. The homeoprotein Nanog is required for maintenance of pluripotency in mouse epiblast and ES cells. Cell 113, 631–642.
Mohn, F., Schübeler, D., 2009. Genetics and epigenetics: stability and plasticity during cellular differentiation. Trends Genet. 25, 129–136.
Mohn, F., Weber, M., Rebhan, M., Roloff, T.C., Richter, J., Stadler, M.B., Bibel, M., Schübeler, D., 2008. Lineage-specific polycomb targets and de novo DNA methylation define restriction and potential of neuronal progenitors. Mol. Cell 30, 755–766.
Mu, Y.M., Oba, K., Yanase, T., Ito, T., Ashida, K., Goto, K., Morinaga, H., Ikuyama, S., Takayanagi, R., Nawata, H., 2003. Human pituitary tumor transforming gene (hPTTG) inhibits human lung cancer A549 cell growth through activation of p21 (WAF1/CIP1). Endocr. J. 50, 771–781.
Murzina, N., Verreault, A., Laue, E., Stillman, B., 1999. Heterochromatin dynamics in mouse cells: interaction between chromatin assembly factor 1 and HP1 proteins. Mol. Cell 4, 529–540.
Nielsen, A.L., Ortiz, J.A., You, J., Oulad-Abdelghani, M., Khechumian, R., Gansmuller, A., Chambon, P., Losson, R., 1999. Interaction with members of the heterochromatin protein 1 (HP1) family and histone deacetylation are differentially involved in transcriptional silencing by members of the TIF1 family. EMBO J. 18, 6385–6395.
Nielsen, A.L., Oulad-Abdelghani, M., Ortiz, J.A., Remboutsika, E., Chambon, P., Losson, R., 2001. Heterochromatin formation in mammalian cells: interaction between histones and HP1 proteins. Mol. Cell 7, 729–739.
O'Geen, H., Squazzo, S.L., Iyengar, S., Blahnik, K., Rinn, J.L., Chang, H.Y., Green, R., Farnham, P.J., 2007. Genome-wide analysis of KAP1 binding suggests autoregulation of KRAB-ZNFs. PLoS Genet. 3, e89.
Quivy, J.P., Gérard, A., Cook, A.J., Roche, D., Almouzni, G., 2008. The HP1-p150/CAF-1 interaction is required for pericentric heterochromatin replication and S-phase progression in mouse cells. Nat. Struct. Mol. Biol. 15, 972–979.
Rambaud, J., Desroches, J., Balsalobre, A., Drouin, J., 2009. TIF1beta/KAP-1 is a coactivator of the orphan nuclear receptor NGFI-B/Nur77. J. Biol. Chem. 284, 14147–14156.
Riclet, R., Chendeb, M., Vonesch, J.L., Koczan, D., Thiesen, H.J., Losson, R., Cammas, F., 2009. Disruption of the interaction between transcriptional intermediary factor 1beta and heterochromatin protein 1 leads to a switch from DNA hyper- to hypomethylation and H3K9 to H3K27 trimethylation on the MEST promoter correlating with gene reactivation. Mol. Biol. Cell 20, 296–305.
Rowe, H.M., Jakobsson, J., Mesnard, D., Rougemont, J., Reynard, S., Aktas, T., Maillard, P.V., Layard-Liesching, H., Verp, S., Marquis, J., Spitz, F., Constam, D.B., Trono, D., 2010. KAP1 controls endogenous retroviruses in embryonic stem cells. Nature 463, 237–240.
Russell, L.D., Ren, H.P., Sinha Hikim, I., Schulze, W., Sinha Hikim, A.P., 1990. A comparative study in twelve mammalian species of volume densities, volumes, and numerical densities of selected testis components, emphasizing those related to the Sertoli cell. Am. J. Anat. 188, 21–30.
Seki, Y., Kurisaki, A., Watanabe-Susaki, K., Nakajima, Y., Nakanishi, M., Arai, Y., Shiota, K., Sugino, H., Asashima, M., 2010. TIF1beta regulates the pluripotency of embryonic stem cells in a phosphorylation-dependent manner. Proc Natl Acad Sci U S A 107, 10926–10931.
Sharpe, R.M., McKinnell, C., Kivlin, C., Fisher, J.S., 2003. Proliferation and functional maturation of Sertoli cells, and their relevance to disorders of testis function in adulthood. Reproduction 125, 769–784.
Smothers, J.F., Henikoff, S., 2000. The HP1 chromo shadow domain binds a consensus peptide pentamer. Curr. Biol. 10, 27–30.
Sripathy, S.P., Stevens, J., Schultz, D.C., 2006. The KAP1 corepressor functions to coordinate the assembly of de novo HP1-demarcated microenvironments of heterochromatin required for KRAB zinc finger protein-mediated transcriptional repression. Mol. Cell. Biol. 26, 8623–8638.
Takizawa, T., Meaburn, K.J., Misteli, T., 2008. The meaning of gene positioning. Cell 135, 9–13.
Thiru, A., Nietlispach, D., Mott, H.R., Okuwaki, M., Lyon, D., Nielsen, P.R., Hirshberg, M., Verreault, A., Murzina, N.V., Laue, E.D., 2004. Structural basis of HP1/PXVXL motif peptide interactions and HP1 localisation to heterochromatin. EMBO J. 23, 489–499.
Tian, C., Xing, G., Xie, P., Lu, K., Nie, J., Wang, J., Li, L., Gao, M., Zhang, L., He, F., 2009. KRAB-type zinc-finger protein Apak specifically regulates p53-dependent apoptosis. Nat. Cell Biol. 11, 580–591.
Tsuruma, R., Ohbayashi, N., Kamitani, S., Ikeda, O., Sato, N., Muromoto, R., Sekine, Y., Oritani, K., Matsuda, T., 2008. Physical and functional interactions between STAT3 and KAP1. Oncogene 27, 3054–3059.
Vergouwen, R.P., Huiskamp, R., Bas, R.J., Roepers-Gajadien, H.L., Davids, J.A., de Rooij, D.G., 1993. Postnatal development of testicular cell populations in mice. J. Reprod. Fertil. 99, 479–485.
Wang, C., Ivanov, A., Chen, L., Fredericks, W.J., Seto, E., Rauscher III, F.J., Chen, J., 2005. MDM2 interaction with nuclear corepressor KAP1 contributes to p53 inactivation. EMBO J. 24, 3279–3290.
Wang, J., Rao, S., Chu, J., Shen, X., Levasseur, D.N., Theunissen, T.W., Orkin, S.H., 2006. A protein interaction network for pluripotency of embryonic stem cells. Nature 444, 364–368.
Wang, C., Rauscher III, F.J., Cress, W.D., Chen, J., 2007. Regulation of E2F1 function by the nuclear corepressor KAP1. J. Biol. Chem. 282, 29902–29909.
Weber, P., Cammas, F., Gerard, C., Metzger, D., Chambon, P., Losson, R., Mark, M., 2002. Germ cell expression of the transcriptional co-repressor TIF1beta is required for the maintenance of spermatogenesis in the mouse. Development 129, 2329–2337.
Wolf, D., Goff, S.P., 2007. TRIM28 mediates primer binding site-targeted silencing of murine leukemia virus in embryonic cells. Cell 131, 46–57.
Wolf, D., Goff, S.P., 2009. Embryonic stem cells use ZFP809 to silence retroviral DNAs. Nature 458, 1201–1204.
Wolf, D., Cammas, F., Losson, R., Goff, S.P., 2008. Primer binding site-dependent restriction of murine leukemia virus requires HP1 binding by TRIM28. J. Virol. 82, 4675–4679.
Ying, H., Furuya, F., Zhao, L., Araki, O., West, B.L., Hanover, J.A., Willingham, M.C., Cheng, S.Y., 2006. Aberrant accumulation of PTTG1 induced by a mutated thyroid hormone beta receptor inhibits mitotic progression. J. Clin. Invest. 116, 2972–2984.